Heparan Sulfate Regulates Intraretinal Axon Pathfinding by Retinal Ganglion Cells

Minako Ogata-Iwao,[1] *Masaru Inatani,*[1] *Keiichiro Iwao,*[1] *Yuji Takihara,*[1] *Yuko Nakaishi-Fukuchi,*[1] *Fumitoshi Irie,*[2] *Shigeru Sato,*[3] *Takahisa Furukawa,*[3] *Yu Yamaguchi,*[2] *and Hidenobu Tanihara*[1]

Purpose. Heparan sulfate (HS) is abundantly expressed in the developing neural retina; however, its role in the intraretinal axon guidance of retinal ganglion cells (RGCs) remains unclear. In this study, the authors examined whether HS was essential for the axon guidance of RGCs toward the optic nerve head.

Methods. The authors conditionally ablated the gene encoding the exostosin-1 (Ext1) enzyme, using the dickkopf homolog 3 (*Dkk3*)-*Cre* transgene, which disrupted HS expression in the mouse retina during directed pathfinding by RGC axons toward the optic nerve head. In situ hybridization, immunohistochemistry, DiI tracing, binding assay, and retinal explant assays were performed to evaluate the phenotypes of the mutants and the roles of HS in intraretinal axon guidance.

Results. Despite no gross abnormality in RGC distribution, the mutant RGC axons exhibited severe intraretinal guidance errors, including optic nerve hypoplasia, ectopic axon penetration through the full thickness of the neural retina and into the subretinal space, and disturbance of the centrifugal projection of RGC axons toward the optic nerve head. These abnormal phenotypes shared similarities with the RGC axon misguidance caused by mutations of genes encoding Netrin-1 and Slit-1/2. Explant assays revealed that the mutant RGCs exhibited disturbed Netrin-1–dependent axon outgrowth and Slit-2–dependent repulsion.

Conclusions. The present study demonstrated that RGC axon projection toward the optic nerve head requires the expression of HS in the neural retina, suggesting that HS in the retina functions as an essential modulator of Netrin-1 and Slit-mediated intraretinal RGC axon guidance. (*Invest Ophthalmol Vis Sci.* 2011;52:6671–6679) DOI:10.1167/iovs.11-7559

From the [1]Department of Ophthalmology and Visual Science, Kumamoto University Graduate School of Medical Sciences, Kumamoto, Japan; the [2]Sanford Children's Health Research Center, Sanford-Burnham Medical Research Institute, La Jolla, California; and the [3]Department of Developmental Biology and JST, CREST, Osaka Bioscience Institute, Osaka, Japan.

Supported by KAKENHI Young Scientists Grant (S) 19679008 from the Ministry of Education, Culture, Sports, Science, and Technology of Japan (MI), National Institutes of Health Grants R01 AR055670 and P01 HD025938 (YY), and Grant-in-Aid for Scientific Research (B) and CREST from the Japan Science and Technology Agency (TF).

Submitted for publication March 15, 2011; revised June 6, 2011; accepted June 21, 2011.

Disclosure: **M. Ogata-Iwao**, None; **M. Inatani**, None; **K. Iwao**, None; **Y. Takihara**, None; **Y. Nakaishi-Fukuchi**, None; **F. Irie**, None; **S. Sato**, None; **T. Furukawa**, None; **Y. Yamaguchi**, None; **H. Tanihara**, None

Corresponding author: Masaru Inatani, Department of Ophthalmology and Visual Science, Kumamoto University Graduate School of Medical Sciences, 1-1-1, Honjo, 860-8556 Kumamoto, Japan; inatani@kumamoto-u.ac.jp.

Retinal ganglion cell (RGC) axons extend outside the eye and convey visual information to the brain. RGC axon projection involves directed, radial pathfinding toward the optic nerve head in the central retina, followed by growth into the optic stalk to form the optic nerve.[1,2] Various guidance molecules play a role. Netrin-1 and its receptor, deleted in colorectal cancer (DCC), control RGC axon growth through the optic nerve head into the optic nerve.[3] Mice lacking *Netrin-1* or *Dcc* exhibit optic nerve hypoplasia because RGC axons fail to reach the optic stalk. Mice lacking ephrin type-B receptor 2 (EphB2) and EphB3 tyrosine kinases contain RGC axons that show guidance errors in the dorsal retina.[4] Antiserum blockade of the immunoglobulin family cell-adhesion molecule L1 results in abnormal intraretinal axon trajectories,[5,6] whereas mice lacking the *L1* gene have no significant intraretinal projection abnormalities.[7] In mice lacking Slit-1 and Slit-2, axon projection toward the optic nerve head was misrouted in RGCs within the peripheral retina.[8] Various guidance molecules appear to participate in intraretinal axon pathfinding by RGCs and compensate for each other.

Proteoglycans are glycosylated proteins that covalently link to the glycosaminoglycans chondroitin sulfate and heparan sulfate (HS), which are abundant in the developing retina.[9,10] Chondroitin sulfate recedes centrifugally in a wavelike fashion toward the peripheral retina during rodent retinal development.[11,12] Enzymatic disturbance of chondroitin sulfate causes aberrant RGC axon orientation in embryonic retinas.[9] The role of HS in intraretinal axon guidance of RGCs has been unclear. We previously generated mice with tissue-specific HS deletions in the developing central nervous system (CNS), in which *nestin*-promoter-driven Cre recombinase removed a *loxP*-modified gene for the HS-synthesizing exostosin-1 (Ext1) enzyme.[13] These mutants exhibited optic nerve-guidance errors in the optic chiasm. We did not evaluate the phenotypes because of late expression of Cre recombinase in the retina after optic nerve head formation. Constitutive loss of *Ext1* results in lethality at embryonic day (E) 7.5 because Ext1 is critical for HS synthesis, polymerizing D-glucuronic acid and *N*-acetyl-D-glucosamine alternatively in the sugar chain backbone.[14] Eliminating enzymes that modify HS chains in vertebrates causes guidance errors in the optic chiasm[15] but has no apparent phenotypic effects on RGC axon-guidance in the retina, suggesting redundancy because of residual HS sugar chains.

To determine the role of HS in intraretinal axon guidance of RGCs, we disrupted *Ext1* in the neural retina before optic nerve formation using the *Dkk3-Cre* transgene, which was expressed as early as E11.5. The HS-deficient retinas exhibited severe guidance errors in RGC axons associated with optic nerve head hypoplasia. The RGC axons failed to respond to Netrin-1– and Slit-2–induced intraretinal axon guidance. These data point to a critical role for HS.

Materials and Methods

Experimental Animals

All the procedures involving mice were performed in accordance with the ARVO Statement for the Use of Animals in Ophthalmic and Vision Research and the guidelines of the Kumamoto University Committee on the Care and Use of Animals. The mutant mouse strains used in this study, including those carrying the *Ext1*^{flox} allele,[13] *Dkk3* promoter-driven *Cre*-transgenic (*Dkk3-Cre*) mice,[16] *Rosa26R* mice,[17] *Nestin* promoter-driven Cre-transgenic (*Nestin-Cre*) mice,[18] and *Netrin-1*–deficient mice,[3] have all been reported previously. To produce mutants with *Ext1*-deficient neural retinas during embryogenesis, *Dkk3-Cre* mice were mated with those carrying the *Ext1*^{flox} allele. Subsequently, to obtain mutants with a *Dkk3-Cre;Ext1*$^{flox/flox}$ genotype, male *Dkk3-Cre;Ext1*$^{flox/wild}$ mice were crossed with females homozygous for the *Ext1*^{flox} allele. Littermates carrying *Ext1*$^{flox/flox}$ or *Ext1*$^{flox/wild}$ without the *Cre* transgene were used as controls. To confirm *Dkk3-Cre*–mediated recombination in the embryonic retina, *Dkk3-Cre* mice were crossed with *Rosa26R* mice (B6; 129-Gt(ROSA)26Sor strain; Jackson Laboratories, Bar Harbor, ME), which expressed β-galactosidase after Cre-mediated recombination. The *Rosa26R* embryos were stained with X-gal (Sigma Chemical, St. Louis, MO). To compare the retinal phenotypes of *Dkk3-Cre;Ext1*$^{flox/flox}$ mutants and mice with *Ext1* disruption mediated by Nestin-Cre, we obtained *Nestin-Cre;Ext1*$^{flox/flox}$ mutants by crossing *Nestin-Cre* mice with those carrying the *Ext1*^{flox} allele, using the method described for the generation of *Dkk3-Cre;Ext1*$^{flox/flox}$ mutants. Genotyping of the mice was performed by polymerase chain reaction–based methods that used DNA prepared from tail biopsy specimens. All the mouse strains were backcrossed with C57BL/6 mice more than 10 times.

In Situ Hybridization

In situ hybridization with a digoxigenin-conjugated riboprobe for the genes encoding the retinal topographic markers ventral anterior homeobox 2 (*Vax2*) and T-box transcription factor 5 (*Tbx5*) was performed in the embryonic retina as described in a previous report,[13] with slight modification. Briefly, whole embryos (E11.5) were incubated with the riboprobe at 55°C overnight, followed by stringent washing. The embryos were then treated with an alkaline phosphatase–conjugated anti–digoxigenin antibody (Roche, Mannheim, Germany). Hybridization signals were visualized with substrate (BM Purple; AP Precipitating Substrate; Roche). A front view of the whole retina was obtained with a stereomicroscope (SZX10; Olympus, Tokyo, Japan).

Histology

Embryos were fixed with Carnoy's fixative solution at 4°C for 3 hours, embedded in paraffin, and processed for histologic examination. After preparing 4-μm-thick sections, samples were stained with hematoxylin and eosin (HE) and then histologically examined under a light microscope. Photographs were taken with a digital camera (DP50; Olympus). To compare the ocular sizes of the *Dkk3-Cre;Ext1*$^{flox/flox}$ embryos and the controls, photoimages of the whole embryos were obtained at E18.5 with a stereomicroscope and then the ocular diameter of the ventrodorsal axis was measured in five embryos from each group.

Immunohistochemistry

Paraffin embedded 4-μm-thick sections fixed with Carnoy's solution, frozen 15-μm-thick sections fixed with 4% paraformaldehyde solution, and flat-mounted retinal sections fixed with 4% paraformaldehyde solution were incubated with primary antibodies. The primary antibodies used were anti–HS, HepSS1 (Seikagaku, Tokyo, Japan), anti–tubulin β-III (Tuj1) (Sigma Chemical), anti–Brn3 (Santa Cruz Biotechnology, Santa Cruz, CA), anti–orthodenticle homeobox 2 (Otx2) (R&D Systems, Minneapolis, MN), anti–Netrin-1 (Abcam, Cambridge, MA), anti–Slit-2 (Abcam), anti–DCC (Santa Cruz Biotechnology), and anti–roundabout-2 (Robo-2) (Abcam). For the diaminobenzidine (DAB) chromogenic reaction, we used biotin-conjugated anti–mouse immunoglobulin (Ig)M (Southern Biotechnology, Birmingham, AL) or anti–goat IgG (Vector, Southfield, MI) secondary antibodies, an ABC kit (Vectastain Elite; Vector) and DAB chromogen (Vector), and mounting solution (Entellan New; Merck, Darmstadt, Germany). Fluorescence immunohistochemistry was performed using Alexa Fluor anti–rabbit or anti–goat secondary antibodies (Molecular Probes, Eugene, OR). After mounting using the antifade reagent (ProLong Gold; Molecular Probes), the sections were examined using a confocal laser microscope (FV300; Olympus). The diameter of the optic nerve head was evaluated after immunohistochemistry for Tuj1 on the sagittal retinal section embedded in paraffin at E14.5. The Tuj1-immunopositve width of the optic nerve head at the level of the retinal pigment epithelium was taken to represent the optic nerve head diameter. The number of RGCs in 4-μm-thick sagittal retinal sections embedded in paraffin was counted after immunohistochemistry for Brn3, which is a marker for embryonic RGCs. The Brn3-immunopositve RGC density in the retinal section was determined by dividing the cell number by the retinal area, which was calculated using bioimaging analysis software (Lumina Vision; Mitani, Fukui, Japan).

DiI Tracing

Crystals of DiI (Invitrogen) were implanted onto the optic nerve head of 4% paraformaldehyde (PFA)-fixed embryos. After 2 weeks' incubation in phosphate-buffered saline (PBS) at 37°C, 500-μm vibratome sections were cut, and the optic nerve projection was examined under a fluorescence microscope. To determine which of the RGC axons projected toward the optic nerve head, they were traced retrogradely by the implantation of DiI onto the retrobulbar optic nerve. After 2 hours of incubation in PBS at 37°C, flat-mounted retinal samples were created. The DiI-labeled RGC axon lengths were measured in each retinal quadrant.

Binding Assay

To study the affinity of guidance molecules for HS, we performed a binding assay that used an enzyme-linked immunosorbent assay (ELISA) method, as previously reported.[19] Briefly, Netrin-1 (R&D Systems), Slit-2 (R&D Systems), basic fibroblast growth factor (bFGF; Wako Pure Chemical, Osaka, Japan), ciliary nerve growth factor (CNTF; PeproTech, Rocky Hill, NJ), and epidermal growth factor (EGF; R&D Systems) were applied to the polystyrene ELISA tray and incubated for 1 hour at 37°C. After blocking with bovine serum albumin (BSA)/PBS, biotinylated HS (Celsus, Cincinnati, OH) was applied to the wells and incubated for 1 hour at 37°C. The bound HS was detected by horseradish peroxidase (HRP)-conjugated streptavidin and an ELISA kit (BioSource/Invitrogen, Carlsbad, CA). Absorbance after the reaction was measured using a plate reader (Model 550; Bio-Rad, Hercules, CA).

ELISA

We performed quantification of HS in Brn3 (a marker for RGCs), Slit-2, Robo-2, Netrin-1 and DCC, in the embryonic retina using enzyme-linked immunosorbent assay (ELISA) at E13.5 (HS ELISA kit; Seikagaku Biobusiness Corporation, Tokyo, Japan). In ELISA for Brn3, Slit-2, Robo-2, Netrin-1, and DCC, embryonic retinal lysate at E13.5 was applied to the polystyrene ELISA tray and was incubated for 1 hour at 37°C. After blocking with BSA/PBS, the primary antibodies were applied to the tray, followed by the incubation with the biotinylated secondary antibodies. After the reaction with HRP-conjugated streptavidin and an ELISA kit (BioSource/Invitrogen), absorbance after the reaction was measured using a plate reader (Model 550; Bio-Rad). The mean ± SE of the values of 450-nm optical density in five retinal samples was shown in each ELISA.

Retinal Explant Assays

Retinal explants were dissected from E13.5 embryos. Explants were cultured for 48 hours in three-dimensional gels of rat tail collagen

(Sigma Chemical) with crosslinked agarose beads (Affi-Gel-Blue; Bio-Rad) absorbed with 50 μg/mL mouse recombinant Netrin-1 (R&D Systems) in 0.1% BSA. For the Slit-2 repulsive assay, a retinal explant (E13.5) was cultured between a Slit-2–transfected 293T cell aggregate and a MOCK-transfected cell aggregate for 48 hours in three-dimensional gels of rat tail collagen. After fixation with 4% PFA, axons were stained with anti–Tuj1 antibody. Immunostaining images were captured with a fluorescence microscope (BZ-8000; Keyence, Osaka, Japan). The total lengths of the Tuj1-positive axon bundles were measured with ImageJ software (developed by Wayne Rasband, National Institutes of Health, Bethesda, MD; available at http://rsb.info.nih.gov/ij/index.html).

Results

Loss of Ext1 and HS in the Neural Retina of *Dkk3-Cre;Ext1$^{flox/flox}$* Embryos

To observe the timing of Cre-driven gene recombination in the *Dkk3-Cre;Ext1$^{flox/flox}$* retina, we crossed *Dkk3-Cre;Ext1$^{flox/flox}$* and *ROSA26R* mice. The resultant *Dkk3-Cre;Ext1$^{flox/flox}$;ROSA26R* mice (Fig. 1A) showed X-gal staining throughout the neural retina at E11.5, when the RGCs started to extend their axons toward the optic nerve head,[20,21] whereas a small population of X-gal–stained cells was initially observed in the E10.5 retina (data not shown). Immunohistochemistry with an anti–HS antibody demonstrated that HS was broadly distributed throughout the ocular tissues, including the neural retina of control embryos at E12.5 (Fig. 1B). Ocular sections of *Dkk3-Cre;Ext1$^{flox/flox}$* embryos revealed little positive staining for the mutant neural retina at E12.5 (Fig. 1C). ELISA for HS showed significantly ($P = 0.0122$) less concentration of HS in the *Dkk3-Cre;Ext1$^{flox/flox}$* retina (0.02 ± 0.01 μg/mL) than in the control retina (0.24 ± 0.11 μg/mL). We confirmed that the optic nerve head in the control embryos started to form on E12.5 (data not shown). These findings indicated that HS synthesis in the *Dkk3-Cre;Ext1$^{flox/flox}$* neural retina had been disrupted before the optic nerve head formation began.

HS Deficiency Caused Optic Nerve Head Hypoplasia

All the mutants died during the first day of life. It was previously reported that neonatal lethality could not be circumvented in conditional gene targeting because some Cre expression was observed in the hippocampus and a part of the cerebral cortex in *Dkk3-Cre* mice.[16] Although the body and eye shapes of *Dkk3-Cre;Ext1$^{flox/flox}$* embryos appeared grossly normal, the ocular size was significantly reduced in the mutants compared with the controls (Figs. 2A–C). A histologic study showed that the mutant retina was associated with a

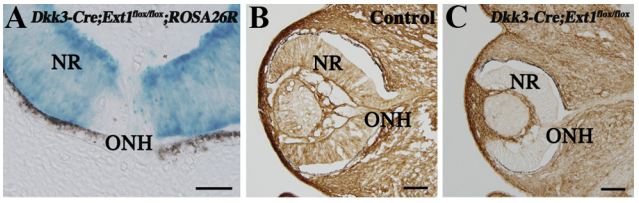

Figure 1. Disrupted expression of HS in the developing neural retina. (**A**) *Dkk3-Cre*-driven recombination in the developing neural retina. Frozen retinal sections of the *Dkk3-Cre;Ext1$^{flox/flox}$;ROSA26R* mutants showed intense β-galactosidase activity throughout the neural retina at E11.5, indicating Cre-driven recombination before the optic nerve head formation. (**B**, **C**) Immunohistochemistry for HS in the control (**B**) and *Dkk3-Cre;Ext1$^{flox/flox}$* (**C**) eyes at E12.5. Note that the HS immunoreactivity had disappeared in the mutant neural retina. NR, neural retina; ONH, optic nerve head. Scale bars, 50 μm.

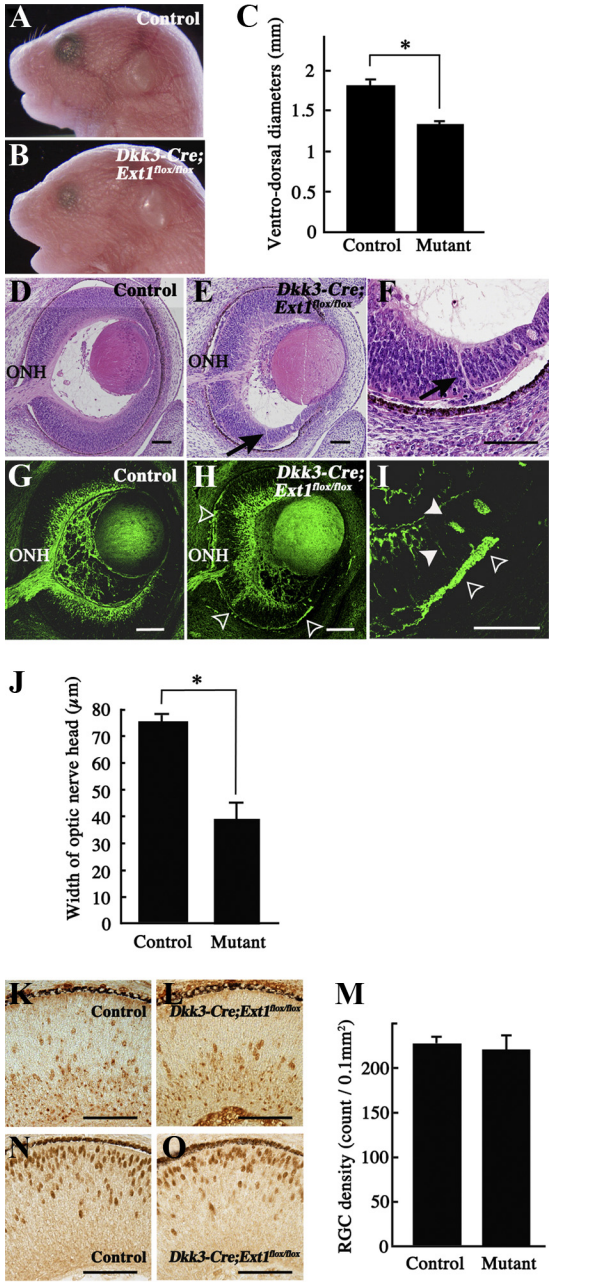

Figure 2. Phenotypes of *Dkk3-Cre;Ext1$^{flox/flox}$* embryos. (**A–C**) Stereomicroscopy of control (**A**) and *Dkk3-Cre;Ext1$^{flox/flox}$* (**B**) embryos at E18.5. The ventrodorsal diameters (**C**) of the *Dkk3-Cre;Ext1$^{flox/flox}$* eyes were significantly smaller than those of the control eyes. Data represent mean ± SE. $^*P <$ 0.001, Wilcoxon signed-rank test ($n = 5$ for each). (**D–F**) HE-stained sagittal sections of the control (**D**) and *Dkk3-Cre;Ext1$^{flox/flox}$* (**E**, **F**) eyes at E14.5. (*arrows*) Ectopic axon bundles that penetrated the full thickness of the mutant peripheral retina. (**G–J**) Tuj1 immunohistochemistry in the control (**G**) and *Dkk3-Cre;Ext1$^{flox/flox}$* (**H**, **I**) eyes at E14.5. *Arrowheads* (**I**) and *open arrowheads* (**H**, **I**) show ectopic axon bundles in the intraretinal region and the subretinal space, respectively. The width (**J**) of the Tuj1-positive optic nerve head of *Dkk3-Cre;Ext1$^{flox/flox}$* mutants was significantly smaller than that of the controls. Data represent mean ± SE $^*P < 0.001$, Wilcoxon signed-rank test ($n = 5$ for each). (**K–M**) Immunohistochemistry for the RGC marker, Brn3, in sagittal sections of the control (**K**) and *Dkk3-Cre;Ext1$^{flox/flox}$* (**L**) eyes at E14.5. There was no significant difference in RGC density between the controls and mutants (**M**). $^*P = 0.7369$, Wilcoxon signed-rank test ($n = 4$ for each). (**N**, **O**) Immunohistochemistry for the photoreceptor cell marker Otx2 in sagittal sections of the control (**N**) and *Dkk3-Cre;Ext1$^{flox/flox}$* (**O**) eyes at E14.5, demonstrating no difference in the distributions. Mutant, *Dkk3-Cre;Ext1$^{flox/flox}$*; ONH, optic nerve head; Scale bars, 50 μm.

smaller optic nerve head (Fig. 2E) than the control retina (Fig. 2D). Staining with anti–Tuj1 antibody confirmed the significantly reduced width of the mutant optic nerve head (Figs. 2G, 2H, 2J). The optic nerve head hypoplasia might have been associated with reduced RGC density in the mutants. We counted the number of RGCs that were stained with anti–Brn3 antibody but found no significant difference between the mutants and the controls in E14.5 sagittal retinal sections (Figs. 2K–M). In addition, ELISA showed no significant difference ($P = 0.6761$) of Brn3 concentration between the control retina (1.22 ± 0.18) and the mutant retina (1.25 ± 0.15). Moreover, immunohistochemistry for Brn3 and Otx2, which is a marker for photoreceptor cells, demonstrated no abnormalities in the localization of specific neuronal populations in the mutant neural retina (Figs. 2K, 2L, 2N, 2O). These results indicated that the reduced size of the mutant optic nerve head was not a secondary consequence of a diminished RGC population or a disturbed distribution of RGC and photoreceptor cells.

HS Deficiency Caused RGC Axon Misguidance within the Retina

HE-stained sagittal sections showed ectopic axon bundles that penetrated the full thickness of the mutant peripheral retina (Fig. 2F). Immunohistochemistry for Tuj1 revealed ectopic axon bundles in the intraretinal region and the subretinal space (Figs. 2H, 2I). Flat-mounted retinal samples revealed further details of the axon-misguidance phenotype of the mutant RGCs. The control RGC axons were radially stained from the peripheral region to the optic nerve head at the level of the nerve fiber layer (Fig. 3A). By contrast, the radially oriented staining of RGC axons was dramatically disturbed in the mutant retinas (Fig. 3B). Most of the stained axons were abnormally oriented in the nasotemporal direction, rather than projecting toward the optic nerve head. At the subretinal level, no Tuj1-positive axons were present in the control retina, except in the retrobulbar part of the optic nerve (Fig. 3C), whereas many ectopic axons were stained at the subretinal level in the mutant flat-mounted retinas (Fig. 3D). These data indicate that the directional projection toward the optic nerve head was disturbed in the mutant RGCs.

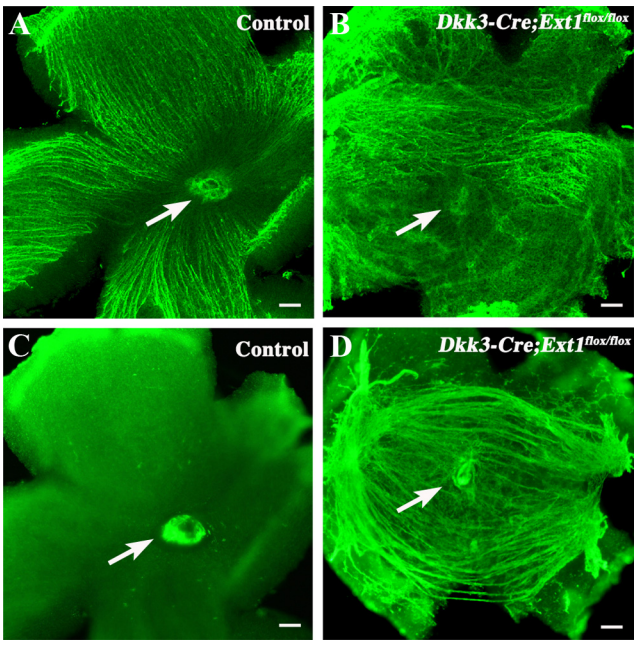

FIGURE 3. Tuj1 immunohistochemistry in flat-mounted retinas. (**A**, **B**) Vitreous side of the flat-mounted retinas of the control (**A**) and *Dkk3-Cre;Ext1*$^{flox/flox}$ (**B**) embryos at E16.5. Note the disturbed projection toward the optic nerve head in the mutant RGC axons. (**C**, **D**) Retinal pigment epithelium side of the flat-mounted retinas of the control (**C**) and *Dkk3-Cre;Ext1*$^{flox/flox}$ (**D**) embryos at E16.5. Numerous ectopic axons were present at the subretinal level of the mutant retina. (*arrows*) Optic nerve head. Scale bars, 50 μm.

HS Deficiency Caused Reduced Projection toward the Optic Nerve Head of RGCs

Retrograde labeling with DiI implantation onto the retrobulbar optic nerve revealed the location of the RGCs with axons extending toward the optic nerve head. As shown in Figures 4C and 4D, the mutant DiI-labeled axons were twisted, whereas the control axons were relatively straight. Retrogradely labeled RGCs were distributed throughout the control flat-mounted retina (Fig. 4A) but were less common in the mutant retina (Fig. 4B). In particular, there were few RGCs in peripheral regions with axons that projected toward the optic nerve head. We compared the total lengths of retrogradely DiI-labeled RGC axons in each quadrant between the mutant and control retinas. The mutant RGCs showed significantly less projection toward the optic nerve head in each quadrant than did the control RGCs (Fig. 4E). However, immunohistochemistry for Brn3 in the flat-mounted retinas demonstrated that RGCs were distributed throughout the mutant (Fig. 4G) and the control (Fig. 4F) samples. In addition, the patterns of expression of the *Vax2* (a marker for ventral retina) and *Tbx5* (a marker for dorsal retina) genes[22] did not differ between the control (Figs. 4H, 4J) and mutant (Figs. 4I, 4K) retinas. These data indicate that a minority of the mutant RGCs projected their axons toward the optic nerve head, even though their distribution and the retinal topography were undisturbed.

Dkk3-Cre;Ext1$^{flox/flox}$ Mutants Had Guidance Errors Similar to Those of Nestin-Cre;Ext1$^{flox/flox}$ Mutants in the Optic Chiasm

Nestin-Cre;Ext1$^{flox/flox}$ mutants showed no abnormal retinal phenotypes such as optic nerve head hypoplasia or ectopic penetration of RGC axons (Figs. 5A, 5B). The some population of retinal cells in *Nestin-Cre;Ext1*$^{flox/flox}$*;ROSA26R* mice showed X-gal staining at E13.5 and E14.5 (Fig. 5C), whereas few X-gal–stained retinal cells were observed until E12.5, suggesting that HS disruption started after the formation of the optic nerve head. Most of the optic nerves have arrived at the optic chiasm by E14.5.[23] Therefore, no abnormal phenotypes were found in the *Nestin-Cre;Ext1*$^{flox/flox}$ mutants, though the retinal axons projected ectopically into the contralateral optic nerve after passage through the optic chiasm.[13] Similarly, the retrobulbar optic nerve of *Dkk3-Cre;Ext1*$^{flox/flox}$ embryos showed ectopic projection into the contralateral optic nerve at the optic chiasm (Fig. 5D).

HS Deficiency Caused Retinal Phenotypes Similar to Netrin-1–Deficient Mutants

The posterior view of the mutant eye demonstrated hypopigmented streaks in the retinal pigment epithelium (Figs. 6A, 6B). Immunohistochemistry for Tuj1 confirmed that these streaks were ectopic axon bundles (Fig. 6C). These phenotypes were also reported previously in *Netrin-1*–deficient mutants.[3] We confirmed that the *Netrin-1*–deficient mutants exhibited not only optic nerve head hypoplasia (Figs. 6D, 6F) but also ectopic penetration through the full thickness of the peripheral retina (Figs. 6E, 6G), thereby showing great similarity to the phenotypes of *Dkk3-Cre;Ext1*$^{flox/flox}$ mutants. However, there were no apparent abnormalities in the distributions of Netrin-1 and DCC in the RGC axons of *Dkk3-Cre;Ext1*$^{flox/flox}$ mutants

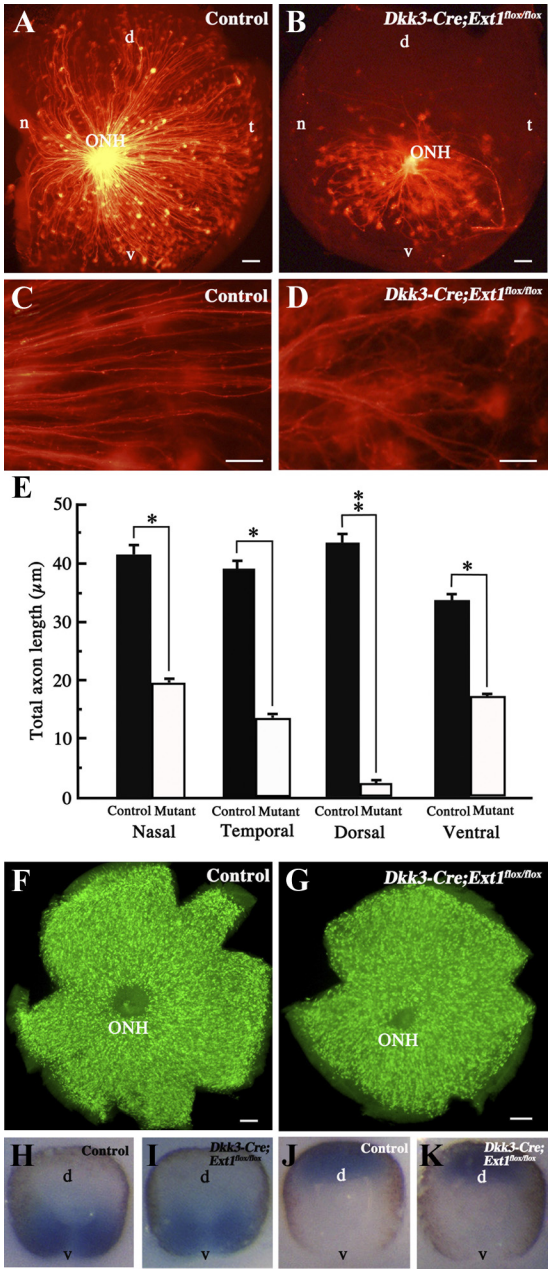

FIGURE 4. Retrograde labeling of RGCs with axons extended toward the optic nerve head. (**A**–**E**) Flat-mounted retinas after retrograde DiI labeling of the control (**A**, **C**) and *Dkk3-Cre;Ext1*$^{flox/flox}$ (**B**, **D**) embryos at E14.5. Fewer axon projections of RGCs toward the optic nerve head were observed in the mutant retina. This reduction was significant in each quadrant (**E**). Data represent mean ± SE. $^{*}P < 0.05$, $^{**}P < 0.01$, Wilcoxon signed-rank test ($n = 5$). The mutant axon projection was twisted (**D**) compared with the controls (**C**). (**F**, **G**) Immunohistochemistry for Brn3 in flat-mounted retina. Brn3-positive cells corresponding to RGCs were distributed throughout the retinas of the controls (**F**) and the mutants (**G**). (**H**–**K**) Whole-mount in situ hybridization for *Vax2* and *Tbx5*. There were no differences in the expression patterns of *Vax2* or *Tbx5* between the control (**H**, *Vax2*; **J**, *Tbx5*) and mutant (**I**, *Vax2*; K, *Tbx5*) retinas. d, dorsal; n, nasal; t, temporal; v, ventral; ONH, optic nerve head. Scale bars, 50 μm.

(Figs. 6H–K). There were no significant differences in the concentrations of Netrin-1 ($P = 0.4034$) or DCC ($P = 0.2101$) between the *Dkk3-Cre;Ext1*$^{flox/flox}$ mutant (2.54 ± 0.30 for Netrin-1 and 1.30 ± 0.19 for DCC) and the control (2.71 ± 0.25 for Netrin-1 and 1.52 ± 0.35 for DCC) retinas. The affinity of Netrin-1 for HS has been recognized since the initial biochemical purification of this axon-guidance molecule.[24,25] In the present study, binding assays confirmed the affinity of Netrin-1 for HS, similar to other HS-binding molecules such as bFGF and Slit-2, whereas EGF and CNTF showed no such activity (Fig. 6L). These results suggest that a loss of HS might disturb Netrin-1–dependent guidance in the retina.

HS Deficiency Caused Loss of Netrin-1–Dependent Outgrowth of RGC Axons In Vitro

To verify that RGC axon guidance depended on the interaction between HS and Netrin-1, we compared RGC axon outgrowth between *Dkk3-Cre;Ext1*$^{flox/flox}$ and control retinal explants in vitro. In the controls, axon outgrowth was notably more robust on Netrin-1–absorbed beads than on BSA-absorbed beads (Fig. 7A), whereas no difference was observed in the mutants (Fig. 7B). The Netrin-1 dependency of axon outgrowth in the control retinal explants was significantly greater than in the mutant retinal explants (Fig. 7C). These data suggest that Netrin-1 requires HS for RGC axon outgrowth in the retina.

Dkk3-Cre;Ext1$^{flox/flox}$ Retinal Explants Lost Slit-2–Dependent Axon Repulsion In Vitro

The failure of axon projection toward the optic nerve head in the *Dkk3-Cre;Ext1*$^{flox/flox}$ mice was similar to the guidance errors reported in the peripheral retina of *Slit-1/2* double-deficient mice.[8] As shown in Figures 8A to 8D, immunohistochemistry demonstrated normal distributions of Slit-2 and its receptor Robo-2, in the *Dkk3-Cre;Ext1*$^{flox/flox}$ retina. There were no significant differences of the concentrations of Slit-2 ($P = 1.0000$) or Robo-2 ($P = 0.6761$) between the *Dkk3-Cre;Ext1*$^{flox/flox}$ mutant (0.11 ± 0.01 for Slit-2 and 1.41 ± 0.64 for Robo-2) and the control (0.11 ± 0.02 for Slit-2 and 1.41 ± 0.44

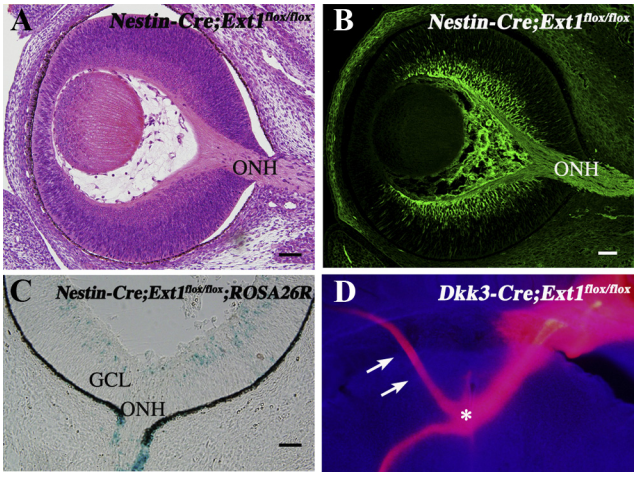

FIGURE 5. Retinal phenotypes in *Nestin-Cre;Ext1*$^{flox/flox}$ mutants. (**A**, **B**) HE-stained (**A**) and Tuj1-immunostained (**B**) sagittal retinal sections at E14.5 demonstrated no optic nerve head hypoplasia or ectopic penetration of RGC axons within the retina. (**C**) X-gal staining in the retinal sample of a *Nestin-Cre;Ext1*$^{flox/flox}$*;ROSA26R* embryo at E14.5. Some retinal cells had β-galactosidase activity, but it was barely detectable in retinal samples up until E12.5, indicating the Cre-driven recombination that was late for the optic nerve formation. (**D**) Ectopic projection into the contralateral optic nerve at the *Dkk3-Cre;Ext1*$^{flox/flox}$ optic chiasm. DiI crystals were implanted onto the optic nerve head of the mutant right eye at E18.5. The anterogradely DiI-labeled optic nerve was misrouted into the optic nerve of the left eye (*arrow*) at the optic chiasm (*asterisk*); this phenotype was observed at the optic chiasm of *Nestin-Cre;Ext1*$^{flox/flox}$ mutants in a previous report.[13] GCL, ganglion cell layer; ONH, optic nerve head. Scale bars, 50 μm.

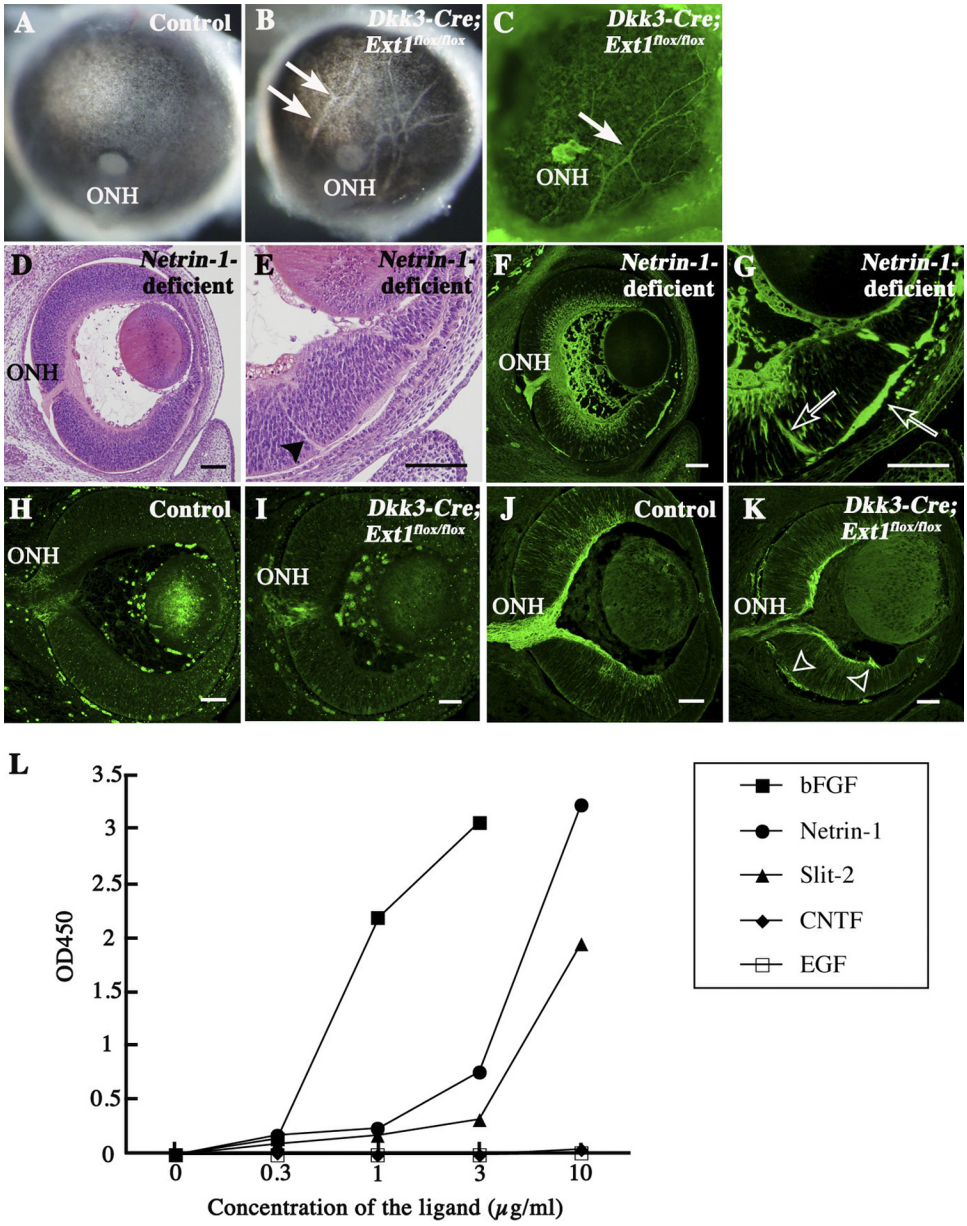

Figure 6. Retinal phenotypes of *Netrin-1*–deficient and *Dkk3-Cre; Ext1*$^{flox/flox}$ mutants. (**A**–**C**) Posterior views of the control (**A**) and *Dkk3-Cre;Ext1*$^{flox/flox}$ (**B**) eyes at E16.5. (*arrows*) Hypopigmented streaks in the retinal pigment epithelium. The streaks in the *Dkk3-Cre;Ext1*$^{flox/flox}$ eyes exhibited Tuj-1 immunoreactivity, suggestive of ectopic axon bundles from the retina (**C**). (**D**, **E**) HE-stained sagittal sections of the *Netrin-1*–deficient retina at E14.5. (**D**, **E**) Optic nerve head hypoplasia was observed. (**E**, *arrowhead)* Ectopic axon bundles. (**F**, **G**) Tuj1 immunohistochemistry in sagittal sections of *Netrin-1*–deficient retina at E14.5. Optic nerve head hypoplasia and ectopic axon bundles (*open arrows*), similar to the phenotypes of *Dkk3-Cre;Ext1*$^{flox/flox}$ mutants, were observed in *Netrin-1*–deficient mutants. (**H**–**K**) Immunohistochemistry for netrin-1 and DCC. In the control retina, Netrin-1 (**H**) and DCC (**J**) immunoreactivities were observed around the optic nerve heads and the RGC axon bundles, respectively. In the *Dkk3-Cre;Ext1*$^{flox/flox}$ retina, netrin-1 (**I**) was also distributed around the hypoplastic optic nerve head. DCC (**K**) in the mutant retina was distributed in the RGC axon bundles and in the ectopic axon bundles (*open arrowheads*). (**L**) HS-binding assay. Netrin-1, bFGF, and Slit-2 bound to HS, whereas EGF and CNTF did not. ONH, optic nerve head. Scale bars, 50 μm.

for Robo-2) retinas. As reported previously,[26] Slit-2 repelled RGC axon outgrowth in control retina explants (Fig. 8E). By contrast, the Slit-2–dependent repulsive effect was significantly disrupted in the *Dkk3-Cre;Ext1*$^{flox/flox}$ retinal explants (Figs. 8F, 8G). These data suggest that the HS-deficient retina exhibited multiple failures of HS-binding molecules in intraretinal RGC axon guidance.

Discussion

The present study examined whether HS was essential for the axon guidance of RGCs toward the optic nerve head. Genetic disruption of *Ext1* in the embryonic neural retina disturbed the axon guidance toward the optic nerve head, causing optic nerve hypoplasia, similar to that seen in *Netrin-1*–deficient and *Slit-1/2*–deficient retinas. An explant assay revealed that the mutant RGCs exhibited disturbed Netrin-1–dependent axon outgrowth and Slit-2–dependent repulsion. Overall, we demonstrated that axon projection of RGCs toward the optic nerve head required the HS expression in the neural retina. These data strongly suggest that HS steers the intraretinal guidance of RGC axons by interactions with Netrin-1 and Slit.

Several previous reports have indicated that HS is critical for projection at the optic chiasm and the optic tract. In *Xenopus*, the exogenous addition of HS to the developing retinotectal pathway prevented retinal axons from entering the optic tectum.[27,28] Mutant mice that lacked *Ext1* in the developing CNS[13] and zebrafish that lacked the genes for HS-modifying enzymes[15] exhibited misguidance at the optic chiasm. However, though these data provided evidence that endogenous HS steered optic nerve outgrowth, they did not reveal abnormal phenotypes for the intraretinal guidance of RGC axons. X-gal staining of the retinal sections of *Nestin-Cre;Ext1*$^{flox/flox}$*; ROSA26R* mice demonstrated that the intraretinal axon-guidance phenotypes could not be evaluated in the mutants because the expression of Cre recombinase in the retina occurred after optic nerve head formation. Moreover, zebrafish mutants for HS-modifying enzymes still expressed HS, though it was less highly sulfated. By contrast, we confirmed gene recombination at E11.5 and a loss of HS at E12.5 in the *Dkk3-Cre;Ext1*$^{flox/flox}$

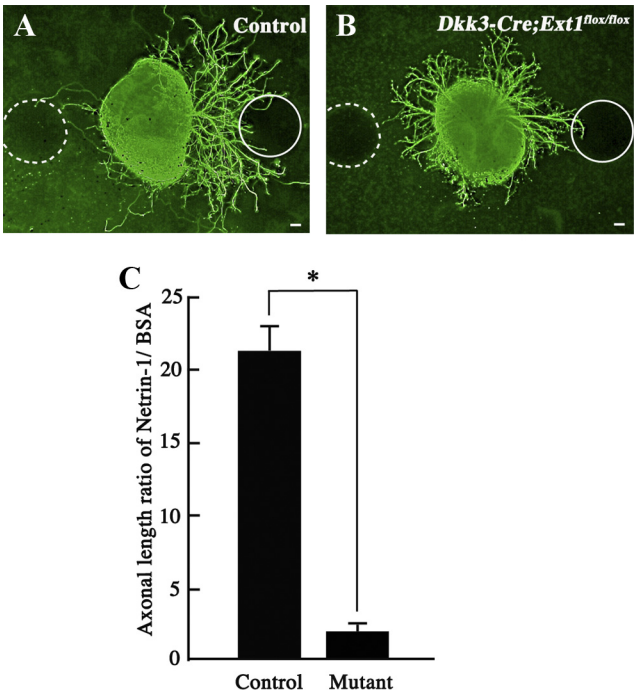

FIGURE 7. Loss of Netrin-1–dependent outgrowth of RGC axons in HS-deficient retinal explants. (**A**) Control retinal explant at E13.5 after 24 hours in vitro. Axon outgrowth was significantly more robust on the Netrin-1–absorbed bead (*solid circle*) than on the BSA-absorbed bead (*broken circle*). (**B**) *Dkk3-Cre;Ext1*$^{flox/flox}$ retinal explant at E13.5 after 24 hours in vitro. The mutant axon outgrowth showed no apparent dependence on Netrin-1. (**C**) The ratio of the total lengths of the axons derived from each aspect was calculated, as indicated in the graph, using the value for the Netrin-1–soaked bead divided by that for the BSA-soaked bead for each explant. The mutant retinal explants showed significantly less dependence on Netrin-1 than the control explants ($n = 29$ for each; $^*P < 0.0001$; Wilcoxon signed-rank test). Mutant, *Dkk3-Cre;Ext1*$^{flox/flox}$. Scale bars, 50 μm.

neural retina, which occurred before optic nerve head formation. The *Dkk3-Cre;Ext1*$^{flox/flox}$ phenotypes thus provide the first evidence of the significance of HS for the intraretinal projection of RGC axons.

Despite severe guidance errors, no gross change in the distribution of RGCs and photoreceptor cells or in retinal topography were found in the *Dkk3-Cre;Ext1*$^{flox/flox}$ retina. No abnormalities in the distribution of these retinal cells was consistent with previous reports about the cerebral cortex phenotypes of *Nestin-Cre;Ext1*$^{flox/flox}$ embryos.[13] These findings indicate that HS plays a substantial role not in the migration of neuronal cells but rather in axon guidance in the retina.

The main abnormal phenotypes of *Dkk3-Cre;Ext1*$^{flox/flox}$ mutants were optic nerve hypoplasia, ectopic axon penetration throughout the full thickness of the neural retina and into the subretinal space, and disturbance of the centrifugal projection of RGC axons to the optic nerve head; these shared features with the phenotypes of mutants disrupted for genes encoding HS-binding guidance molecules. HS has been shown to interact with Slit/Robo,[29] Netrin-1/DCC,[30] and Semaphorin/Plexin[31] axon-navigation systems. *Netrin-1*–deficient mutants have been associated with optic nerve hypoplasia and ectopic axon penetration through the full thickness of the neural retina and into the subretinal space. Hypopigmented streaks in the retinal pigment epithelium corresponding to ectopic axon bundles have also been observed in *Netrin-1*–deficient eyes. These similarities suggest a disturbance of Netrin-1/DCC signaling in the *Dkk3-Cre;Ext1*$^{flox/flox}$ retina. Netrin-1 induced RGC axon

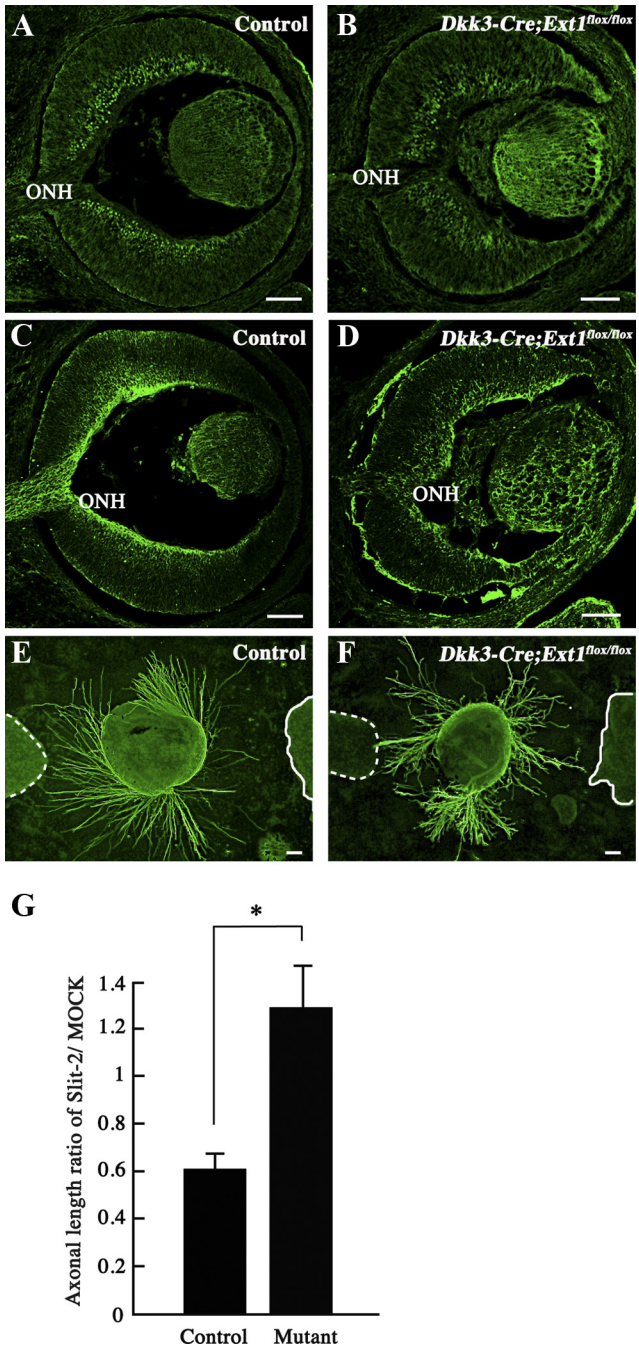

FIGURE 8. Loss of the Slit-2–dependent repulsive effect of RGC axons in the HS-deficient retinal explants. (**A–D**) Immunohistochemistry for Slit-2 and Robo-2. In the control retina, Slit-2 (**A**) and Robo-2 (**C**) immunoreactivities were observed in the inner region of the neural retina and in the RGC axon bundles including the optic nerve head, respectively. In the *Dkk3-Cre;Ext1*$^{flox/flox}$ retina, Slit-2 (**B**) was also distributed in the inner region of the neural retina. Robo-2 (**D**) in the mutant retina was distributed in the RGC axon bundles and the ectopic axon bundles. (**E–G**) Slit-2–induced chemorepulsive assay for axon outgrowth from a retinal explant (48 hours in vitro at E13.5). Axon outgrowth from the control explant (**E**) was repelled in the Slit-2–transected 293T cell aggregate (*solid line*), whereas the *Dkk3-Cre;Ext1*$^{flox/flox}$ axons (**F**) showed no repulsion in the Slit-2–transfected cell aggregate (*solid line*). (*broken lines*) Mock-transfected 293T cell aggregates. Statistical analysis (**G**) confirmed significantly less dependence on Slit-2 in the mutant retinal explants than in the control explants ($n = 21$ for control and $n = 24$ for *Dkk3-Cre;Ext1*$^{flox/flox}$; $^*P = 0.0002$; Wilcoxon signed-rank test). Mutant, *Dkk3-Cre;Ext1*$^{flox/flox}$; ONH, optic nerve head. Scale bars, 50 μm.

outgrowth in vitro.[3,32] The interaction between HS and Netrin-1 induced axon outgrowth in the commissural neurons of the spinal cord[30] and diencephalospinal longitudinal tract formation of dopaminergic neurons in the posterior tuberculum of zebrafish.[33] In the present study, HS-deficient retinal explants did not show Netrin-1–dependent axon outgrowth in vitro, suggesting disturbed Netrin-1/DCC signaling in the *Dkk3-Cre;Ext1*$^{flox/flox}$ retina. Taken together, these data suggest that the interaction between HS and Netrin-1 promotes optic nerve formation, thereby preventing the ectopic penetration of RGC axons.

The axon misguidance observed in the *Dkk3-Cre;Ext1*$^{flox/flox}$ retina was more severe than that in the *Netrin-1*–deficient retina. Most of the mutant RGC axons in the optic fiber layer of the peripheral retinal region projected straight toward the optic nerve head in *Netrin-1*–deficient mutants,[3] whereas the axon projection toward the optic nerve head in the peripheral retinal region of *Dkk3-Cre;Ext1*$^{flox/flox}$ mutants was more drastically disturbed, indicating the possibility of the disturbed functioning of another guidance molecule. In *Slit-1/2*–deficient retinas, some of the RGC axon bundles extend ectopically into the outer retinal layers, escaping from the optic fiber layer: 25% of the RGC axons originating in the periphery of the retina deviate from their normal peripheral-central orientation and form abnormal curved trajectories.[8] Slit-1 and Slit-2, which are expressed in the neural retina and the lens, are thought to mediate the axon projection of RGCs to the optic nerve head, exerting a chemorepulsive effect. By contrast, the present explant assay demonstrated that RGC axons from the *Dkk3-Cre;Ext1*$^{flox/flox}$ retinal explants failed to repel from Slit-2–expressing 293T cells. In addition, in guidance events other than intraretinal projection, a loss of HS reportedly disturbs Slit-dependent axon guidance.[13,34–38] This evidence suggests that the axon projection of RGCs toward the optic nerve head in the *Dkk3-Cre;Ext1*$^{flox/flox}$ retina might be impaired through Slit/Robo signaling; hence, the intraretinal guidance errors observed in *Dkk3-Cre;Ext1*$^{flox/flox}$ eyes might be compound phenocopies of *netrin-1* and *slit-1/2* mutants.

We could not discount the possibility that other HS-binding guidance molecules were also affected in the *Dkk3-Cre;Ext1*$^{flox/flox}$ retina. Ephrin-A3[39] and ephrin-B3[40] have binding sites for HS. Ephrin-A3–deficient mutants and triple-knockout mice, including the genes for ephrin-A2 and ephrin-A5, exhibit disturbances of retinogeniculate and retinocollicular projection, though no apparent misguidance has been reported in intraretinal axon projection. Mutant mice lacking genes for both EphB2 and EphB3, which are receptors for ephrin-B3, show RGC axon-pathfinding errors; however, the incidence is 33% in the mutants, and only a few axons diverge from the normal projection toward the optic nerve head.[4] This phenotypic difference indicates that RGC axon misguidance in the *Dkk3-Cre;Ext1*$^{flox/flox}$ retina cannot be adequately explained by the disturbance of the interaction between HS and ephirin-A3 or ephirin-B3.

The present retinal explant assay strongly suggested that HS originating from RGCs affected the Netrin-1- and Slit-2–dependent axon guidance of RGCs. HS controls HS-binding molecules through two modes of action. First, HS modulates the diffusion and the gradient of HS-binding molecules within the local environment. In *Drosophila*, HS regulates the gradient formation of transforming growth factor-β (TGF-β) and Wnt homologs during wing development.[41,42] However, the present study revealed no changes to the distributions of Netrin-1 and Slit-2 in the mutant retina. Second, HS proteoglycans on the RGC axons promote the interactions between guidance molecules and receptors. The enzymatic digestion of HS abolishes the chemorepulsive response to Slit-2 in olfactory interneuron precursors[29] and *Xenopus* retinal axons.[43] We previously reported that HS-deficient commissural neurons showed abnormal projection in the spinal cord, where HS was expressed normally.[30] Moreover, the present in vitro study confirmed that HS-deficient retinal explants had lost the axon response to Netrin-1 or Slit-2. HS-deficient RGCs also exhibited abnormal axon guidance in the optic chiasm, but this local environment expressed HS normally. These findings are consistent with the concept that HS proteoglycans on the axon surface regulate guidance signals through the interactions between HS and guidance molecules.[44]

In conclusion, we demonstrated that HS was an essential factor for the intraretinal projection of RGC axons. HS deficiency led to severe guidance errors, such as optic nerve head hypoplasia, ectopic axon penetration into the full thickness of the neural retina and the subretinal space, and disturbance of the directional projection toward the optic nerve head, which were composites of those caused by losses of Netrin-1 and Slit-2. HS appeared to modulate the proper function of these HS-binding guidance molecules in RGC axon projection during intraretinal axon pathfinding.

Acknowledgments

The authors thank H. Okita and P. Soriano for the Rosa26R mice; Marc Tessier-Lavigne for the Netrin-1–deficient mice; Yasuhide Furuta for the *Vax2* and *Tbx5* plasmids; Kunimasa Ohta, Yohei Shinmyo, and Hideaki Tanaka for experimental advice; and Chika Naito and Mao Miyagawa for experimental assistance.

References

1. Harada T, Harada C, Parada LF. Molecular regulation of visual system development: more than meets the eye. *Genes Dev.* 2007; 21:367–378.
2. Inatani M. Molecular mechanisms of optic axon guidance. *Naturwissenschaften.* 2005;92:549–561.
3. Deiner MS, Kennedy TE, Fazeli A, Serafini T, Tessier-Lavigne M, Sretavan DW. Netrin-1 and DCC mediate axon guidance locally at the optic disc: loss of function leads to optic nerve hypoplasia. *Neuron.* 1997;19:575–589.
4. Birgbauer E, Cowan CA, Sretavan DW, Henkemeyer M. Kinase independent function of EphB receptors in retinal axon pathfinding to the optic disc from dorsal but not ventral retina. *Development.* 2000;127:1231–1241.
5. Bastmeyer M, Ott H, Leppert CA, Stuermer CA. Fish E587 glycoprotein, a member of the L1 family of cell adhesion molecules, participates in axonal fasciculation and the age-related order of ganglion cell axons in the goldfish retina. *J Cell Biol.* 1995;130: 969–976.
6. Brittis PA, Lemmon V, Rutishauser U, Silver J. Unique changes of ganglion cell growth cone behavior following cell adhesion molecule perturbations: a time-lapse study of the living retina. *Mol Cell Neurosci.* 1995;6:433–449.
7. Demyanenko GP, Maness PF. The L1 cell adhesion molecule is essential for topographic mapping of retinal axons. *J Neurosci.* 2003;23:530–538.
8. Thompson H, Camand O, Barker D, Erskine L. Slit proteins regulate distinct aspects of retinal ganglion cell axon guidance within dorsal and ventral retina. *J Neurosci.* 2006;26:8082–8091.
9. Brittis PA, Canning DR, Silver J. Chondroitin sulfate as a regulator of neuronal patterning in the retina. *Science.* 1992;255:733–736.
10. Koga T, Inatani M, Hirata A, et al. Expression of glycosaminoglycans during development of the rat retina. *Curr Eye Res.* 2003;27: 75–83.
11. Brittis PA, Silver J. Multiple factors govern intraretinal axon guidance: a time-lapse study. *Mol Cell Neurosci.* 1995;6:413–432.
12. Chung KY, Shum DK, Chan SO. Expression of chondroitin sulfate proteoglycans in the chiasm of mouse embryos. *J Comp Neurol.* 2000;417:153–163.
13. Inatani M, Irie F, Plump AS, Tessier-Lavigne M, Yamaguchi Y. Mammalian brain morphogenesis and midline axon guidance require heparan sulfate. *Science.* 2003;302:1044–1046.

14. Lin X, Wei G, Shi Z, et al. Disruption of gastrulation and heparan sulfate biosynthesis in EXT1-deficient mice. *Dev Biol.* 2000;224: 299–311.
15. Pratt T, Conway CD, Tian NM, Price DJ, Mason JO. Heparan sulphation patterns generated by specific heparan sulfotransferase enzymes direct distinct aspects of retinal axon guidance at the optic chiasm. *J Neurosci.* 2006;26:6911–6923.
16. Sato S, Inoue T, Terada K, et al. Dkk3-Cre BAC transgenic mouse line: a tool for highly efficient gene deletion in retinal progenitor cells. *Genesis.* 2007;45:502–507.
17. Soriano P. Generalized lacZ expression with the ROSA26 Cre reporter strain. *Nat Genet.* 1999;21:70–71.
18. Tronche F, Kellendonk C, Kretz O, et al. Disruption of the glucocorticoid receptor gene in the nervous system results in reduced anxiety. *Nat Genet.* 1999;23:99–103.
19. Pankhurst GJ, Bennett CA, Easterbrook-Smith SB. Characterization of the heparin-binding properties of human clusterin. *Biochemistry.* 1998;37:4823–4830.
20. Dräger UC. Birth dates of retinal ganglion cells giving rise to the crossed and uncrossed optic projections in the mouse. *Proc R Soc Lond B Biol Sci.* 1985;224:57–77.
21. Silver J, Sidman RL. A mechanism for the guidance and topographic patterning of retinal ganglion cell axons. *J Comp Neurol.* 1980;189:101–111.
22. Schulte D, Furukawa T, Peters MA, Kozak CA, Cepko CL. Misexpression of the Emx-related homeobox genes cVax and mVax2 ventralizes the retina and perturbs the retinotectal map. *Neuron.* 1999;24:541–553.
23. Colello RJ, Guillery RW. The early development of retinal ganglion cells with uncrossed axons in the mouse: retinal position and axonal course. *Development.* 1990;108:515–523.
24. Kennedy TE, Serafini T, de la Torre JR, Tessier-Lavigne M. Netrins are diffusible chemotropic factors for commissural axons in the embryonic spinal cord. *Cell.* 1994;78:425–435.
25. Serafini T, Kennedy TE, Galko MJ, Mirzayan C, Jessell TM, Tessier-Lavigne M. The netrins define a family of axon outgrowth-promoting proteins homologous to *C. elegans* UNC-6. *Cell.* 1994;78:409–424.
26. Niclou SP, Jia L, Raper JA. Slit-2 is a repellent for retinal ganglion cell axons. *J Neurosci.* 2000;20:4962–4974.
27. Irie A, Yates EA, Turnbull JE, Holt CE. Specific heparan sulfate structures involved in retinal axon targeting. *Development.* 2002; 129:61–70.
28. Walz A, McFarlane S, Brickman YG, Nurcombe V, Bartlett PF, Holt CE. Essential role of heparan sulfates in axon navigation and targeting in the developing visual system. *Development.* 1997;124: 2421–2430.
29. Hu H. Cell-surface heparan sulfate is involved in the repulsive guidance activities of Slit-2 protein. *Nat Neurosci.* 2001;4:695–701.
30. Matsumoto Y, Irie F, Inatani M, Tessier-Lavigne M, Yamaguchi Y. Netrin-1/DCC signaling in commissural axon guidance requires cell-autonomous expression of heparan sulfate. *J Neurosci.* 2007; 27:4342–4350.
31. Kantor DB, Chivatakarn O, Peer KL, et al. Semaphorin 5A is a bifunctional axon guidance cue regulated by heparan and chondroitin sulfate proteoglycans. *Neuron.* 2004;44:961–975.
32. de la Torre JR, Hopker VH, Ming GL, et al. Turning of retinal growth cones in a netrin-1 gradient mediated by the netrin receptor DCC. *Neuron.* 1997;19:1211–1224.
33. Kastenhuber E, Kern U, Bonkowsky JL, Chien CB, Driever W, Schweitzer J. Netrin-DCC, Robo-Slit, and heparan sulfate proteoglycans coordinate lateral positioning of longitudinal dopaminergic diencephalospinal axons. *J Neurosci.* 2009;29:8914–8926.
34. Bülow HE, Hobert O. Differential sulfations and epimerization define heparan sulfate specificity in nervous system development. *Neuron.* 2004;41:723–736.
35. Johnson KG, Ghose A, Epstein E, Lincecum J, O'Connor MB, Van Vactor D. Axonal heparan sulfate proteoglycans regulate the distribution and efficiency of the repellent slit during midline axon guidance. *Curr Biol.* 2004;14:499–504.
36. Lee JS, von der Hardt S, Rusch MA, et al. Axon sorting in the optic tract requires HSPG synthesis by ext2 (dackel) and extl3 (boxer). *Neuron.* 2004;44:947–960.
37. Rhiner C, Gysi S, Frohli E, Hengartner MO, Hajnal A. Syndecan regulates cell migration and axon guidance in *C. elegans*. *Development.* 2005;132:4621–4633.
38. Steigemann P, Molitor A, Fellert S, Jackle H, Vorbruggen G. Heparan sulfate proteoglycan syndecan promotes axonal and myotube guidance by slit/robo signaling. *Curr Biol.* 2004;14:225–230.
39. Irie F, Okuno M, Matsumoto K, Pasquale EB, Yamaguchi Y. Heparan sulfate regulates ephrin-A3/EphA receptor signaling. *Proc Natl Acad Sci U S A.* 2008;105:12307–12312.
40. Holen HL, Zernichow L, Fjelland KE, et al. Ephrin-B3 binds to a sulfated cell surface receptor. *Biochem J.* 2010;433:215–223.
41. Belenkaya TY, Han C, Yan D, et al. *Drosophila* Dpp morphogen movement is independent of dynamin-mediated endocytosis but regulated by the glypican members of heparan sulfate proteoglycans. *Cell.* 2004;119:231–244.
42. Kleinschmit A, Koyama T, Dejima K, Hayashi Y, Kamimura K, Nakato H. *Drosophila* heparan sulfate 6-O endosulfatase regulates Wingless morphogen gradient formation. *Dev Biol.* 2010;345: 204–214.
43. Hussain SA, Piper M, Fukuhara N, et al. A molecular mechanism for the heparan sulfate dependence of slit-robo signaling. *J Biol Chem.* 2006;281:39693–39698.
44. Rhiner C, Hengartner MO. Sugar antennae for guidance signals: syndecans and glypicans integrate directional cues for navigating neurons. *Scientific World Journal.* 2006;6:1024–1036.